Anharmonic Phonon Lifetimes in Semiconductors from Density-Functional Perturbation Theory

Alberto Debernardi,[1,2] Stefano Baroni,[1,2,3] and Elisa Molinari[1,4]
[1]*Istituto Nazionale di Fisica della Materia (INFM)*
[2]*Scuola Internazionale Superiore di Studi Avanzati (SISSA), Via Beirut 2-4, 34014 Trieste, Italy*
[3]*Centre Européen de Calcul Atomique et Moleculaire (CECAM), ENS-Lyon, 46 Allée d'Italie, 69007 Lyon, France*
[4]*Dipartimento di Fisica, Università di Modena, Via Campi 213/a, I-41100 Modena, Italy*
(Received 14 April 1995)

The anharmonic lifetimes of zone-center optical phonons in C, Si, and Ge are calculated along with their temperature and pressure dependences, using third-order density-functional perturbation theory. Our basic ingredients are by-products of a standard linear-response calculation of phonon dispersions in the harmonic approximation, resulting in a similarly good agreement with experiments. The microscopic mechanisms responsible for the decay are revealed and shown to be different for different materials and to depend sensitively on the applied pressure.

PACS numbers: 63.20.Ry, 31.15.Ar, 31.15.Ew, 36.20.Ng

The anharmonic decay of phonons into vibrations of lower frequency is a crucial mechanism for energy relaxation in semiconductors as it controls the formation and time evolution of nonequilibrium (*hot*) phonon populations, which are emitted by high-density excited carriers when they decay towards their ground state [1]. Many technologically important processes in which electrons are excited high into the conduction band—either optically or by an applied electric field—can be influenced by the presence of hot phonons because these can be reabsorbed by electrons, thus leading to a much slower relaxation of the whole system towards equilibrium [2].

Experimentally, anharmonic lifetimes of individual zone-center phonons can be extracted from their measured Raman linewidths, if inhomogeneous broadening effects can be neglected. Menéndez and Cardona have obtained the full temperature dependence for elemental semiconductors more than a decade ago [3]. This is, however, much more difficult in systems, such as heterostructures, where composition or strain inhomogeneities add to the usual (e.g., isotopic [4]) broadening factors. Experiments in the time domain by ultrafast spectroscopies have also become available in recent years, but their interpretation is often not straightforward, especially in complex structures, owing to the coupling between the dynamics of carrier and phonon populations [1].

In this Letter we show that anharmonic lifetimes of semiconductors can be determined within a predictive theoretical scheme, allowing a full understanding of the detailed microscopic processes that lead to phonon decay. Previous studies in this field were based on strong simplifications of the possible mechanisms—as in the early paper by Klemens that only considered decay processes into two phonons of equal frequency [5]—and/or on simplified phenomenological models for describing harmonic and anharmonic interactions [6]. The only previous attempt to apply *ab initio* techniques to the anharmonic decay of phonons was done for Si using a semiempirical lattice-dynamical model fitted to a few frozen-phonon calculations [7]. As a result, the available theoretical estimates for bulk elemental semiconductors show a huge spread, and their ability to account for experimental findings is rather questionable: In Ref. [3], Menéndez and Cardona have provided a comprehensive discussion of the limitations of previous theoretical work, pointing out the critical ingredients that need to be taken into account for reliable predictions. We have developed a new first-principles approach to anharmonic decay of phonons, based on density-functional perturbation theory [8–10], which in recent years has proved to be a very accurate and predictive tool for the study of vibrations in semiconductors [9,11,12]. The crucial step is that third-order perturbation theory [10] can be used efficiently [13], and can be implemented using ingredients which are by-products of standard *ab initio* lattice-dynamical calculations in the harmonic approximation [9,10,13], thus requiring a similar computational effort and resulting in a similar accuracy. Our method is demonstrated by calculating the phonon lifetimes in diamond, Si, and Ge, along with their temperature and pressure dependence. Our results, which are in good agreement with available experimental data, allow a clear understanding of the relative importance of different decay mechanisms, and open the possibility to study modifications of lifetimes that can be induced through external parameters (such as, e.g., pressure and materials engineering) affecting the efficiency of individual decay channels.

If only three-phonon processes are considered, energy and momentum conservation dictate that the zone-center

0031-9007/95/75(9)/1819(4)$06.00

LTO phonon decays into a pair of phonons with opposite momenta, $\pm\mathbf{q}$, whose frequencies sum up to the frequency of the decaying mode. Following Ref. [3], the inverse lifetime Γ of the LTO mode at zone center reads

$$\Gamma = \frac{\pi\hbar}{16N^3M^3\omega_{\mathrm{LTO}}(\mathbf{0})} \sum_{\mathbf{q},j_1,j_2} \left(\frac{\partial^3 E}{\partial u_{\mathrm{LTO}}(\mathbf{0})\partial u_{j_1}(\mathbf{q})\partial u_{j_2}(-\mathbf{q})} \right)^2 \times \frac{n_{j_1}(\mathbf{q}) + n_{j_2}(-\mathbf{q}) + 1}{\omega_{j_1}(\mathbf{q})\omega_{j_2}(-\mathbf{q})} \times \delta(\omega_{\mathrm{LTO}}(\mathbf{0}) - \omega_{j_1}(\mathbf{q}) - \omega_{j_2}(-\mathbf{q})), \quad (1)$$

where N is the number of unit cells in the crystal, M is the atomic mass, the ω's are phonon frequencies, the n's are the thermal occupation numbers, the j's indicate the phonon branches ($j = 1-6$ in bulk elemental semiconductors), E is the crystal energy, and $u_j(\mathbf{q})$ is the amplitude of the jth phonon mode at wave vector $\mathbf{q}$. Besides the ω's and u's, which are immediately available from a lattice-dynamical calculation in the harmonic approximation, the new quantities that need to be evaluated are the third derivatives of the crystal energy with respect to atomic displacements. The latter are obtained using the method proposed in Ref. [13] and based on the so-called $2n + 1$ theorem, which ensures that the knowledge of the electronic wave function response of a system up to order n in the strength of an external perturbation is sufficient to determine the energy derivatives with respect to the strength up to order $2n + 1$ [10,14]. For $n = 1$, this theorem implies that third-order anharmonic couplings can be calculated from the *linear* response of the electron wave function to lattice distortions, hence from the same ingredients that enter standard lattice-dynamical calculations in the harmonic approximation [9]. Calculations were performed within density-functional theory in the local-density approximation, using the plane-wave pseudopotential method. Our basis sets are truncated to a kinetic-energy cutoff of 22 Ry for Si and Ge and to 55 Ry for C. The pseudopotentials used as well as other technical details are the same as in Refs. [9] and [12]. The sum over the $\mathbf{q}$ points appearing in Eq. (1) is performed by the tetrahedron method, using approximately 1500 tetrahedra in the irreducible wedge of the Brillouin zone. The nonsingular part of the integrand is calculated on a much coarser uniform mesh and then Fourier interpolated on the finer grid, much in the same way as phonon dispersions are obtained from selected calculations on a relatively coarse grid, passing through interatomic force constants [9].

The calculated low-temperature linewidths of the LTO phonons in C, Si, and Ge are reported in Table I [15], together with selected experimental data from Raman scattering experiments. Although the spread in the published experimental results is rather large [16–18]—ranging from 1.2 to 2.9 cm^{-1} for C, from 1.24 to 2.1 cm^{-1} for Si, and from 0.75 to 1.4 cm^{-1} for Ge—we can conclude that the agreement is good.

To identify the relevant processes contributing to these results, in Table I we also report the relative weight of individual decay channels, obtained by restricting the sums over the j's in Eq. (1) to selected final states: "TA" ($j = 1, 2$) and "LA" ($j = 3$). The decay into one optical and one acoustic phonon is kinematically forbidden in all the present cases. It turns out that the dominant decay mechanisms are not the same in the three semiconductors. In Si and Ge, the process with maximum probability ($\simeq$95%) involves one LA and and one TA mode as final states, and the *Klemens channel*, i.e., the decay of the LTO mode into two acoustic phonons belonging to a same branch and with opposite momenta, turns out to give a very small contribution. In diamond, instead, the Klemens channels—TA + TA ($\simeq$31%) and LA + LA ($\simeq$15%)—become dominant at the expense of the LA + TA channel. This analysis is made more clear by defining the *frequency-resolved final state spectrum*, $\gamma(\omega)$, i.e., the probability per unit time that the LTO phonon decays into one mode of given frequency ω and one of frequency $\omega_{\mathrm{LTO}} - \omega$. In practice, $\gamma(\omega)$ is obtained by restricting the sum over j_1 and $\mathbf{q}$ in Eq. (1) to those values for which $\omega_{j_1}(\mathbf{q}) = \omega$, by inserting $\delta(\omega - \omega_{j_1}(\mathbf{q}))$ under the sign of the sum. By its definition, $\gamma(\omega)$ is symmetric around $\omega_{\mathrm{LTO}}/2$ and normalized to Γ. In Fig. 1 we display $\gamma(\omega)$, as calculated at $T = 0$ for the three materials considered in this work. The peak at $\omega_{\mathrm{LTO}}/2$ corresponds to the Klemens decay mechanism. As anticipated in Table I, this peak is dominant only in diamond. By comparison with the one-phonon density of states (DOS)—dashed lines in Fig. 1, we realize that this occurs because diamond is the only case where $\omega_{\mathrm{LTO}}/2$ falls in a region of relatively large DOS [between TA(L) and TA(X) [12]]. The lateral peaks, symmetric with respect to $\omega_{\mathrm{LTO}}/2$, are instead dominant for Si and Ge.

In Fig. 2 we display the temperature dependence of the Raman linewidths in diamond, Si, and Ge, as obtained by

TABLE I. Calculated full widths at half maximum (2Γ) of zone-center optical phonons at zero temperature and pressure. The corresponding experimental values are shown for comparison. The last columns indicate the relative contributions to the linewidth of the individual decay channels (see text).

	2Γ (cm^{-1})	2Γ(expt.) (cm^{-1})	LA + LA (%)	LA + TA (%)	TA + TA (%)
C	1.01	1.2[a]	14.7	33.9	30.7[b] + 20.7
Si	1.48	1.45[c]	6.0	94.0	
Ge	0.67	0.75[d]	4.6	95.4	

[a]From Ref. [16].
[b]*Klemens channel*, see text.
[c]From Ref. [17(c)].
[d]From Ref. [3].

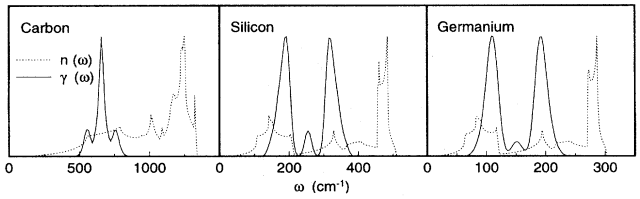

FIG. 1. Calculated phonon density of states, $n(\omega)$ (solid line), and frequency-resolved final state spectra, $\gamma(\omega)$ (dashed line), for the three elemental semiconductors C, Si, and Ge at zero temperature and pressure.

including the appropriate thermal phonon occupation numbers in Eq. (1). The agreement with experiments is very good. The only deviations occur above $T \sim \hbar\omega_{\mathrm{LTO}}/k_B$, i.e., far above room temperature, where higher-order anharmonic terms are likely to account for the discrepancies.

In Fig. 3 we report our predictions for the pressure dependence of the Raman linewidths, as obtained by performing the same calculations for the diamond structure at different values of the crystal volume. For Ge, the results above 110 kbar are not physical because a structural phase transition occurs at this pressure. The pressure dependence is relatively featureless for diamond, whereas it is roughly characterized by a linear behavior for Si and Ge. The slope of this linear dependence, however, displays a rather well defined discontinuity at some critical pressures $P^\star$ ($P^\star \approx 70$–80 and 120–130 kbar, for Si and Ge, respectively).

In order to get a deeper insight into the microscopic mechanisms that determine the decay process and its pressure dependence, we plot in Fig. 4 the *wave vector-resolved final state spectrum*, i.e., the $\mathbf{q}$-dependent function that appears in Eq. (1) under the sign of the sum. Because of energy conservation, as expressed by the δ function, this quantity is different from zero only on a 3D surface of which we display the intersection with some high-symmetry planes in the Brillouin zone (BZ). The magnitude of the function on that surface (i.e., the magnitude of the matrix element responsible for the phonon decay) is represented by a color scale going from red to violet in order of increasing magnitude. Let us focus on Fig. 4(b) (zero pressure). Again, it is easy to identify the contribution of Klemens processes in the closed contour

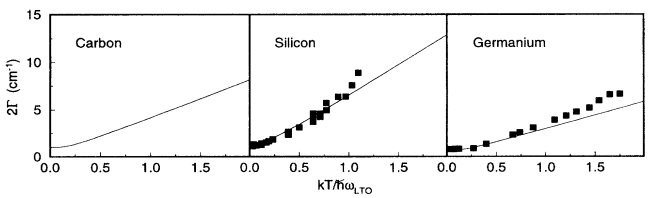

FIG. 2. Temperature dependence of the full width at half maximum, 2Γ, of the LTO phonon in C, Si, and Ge. Solid lines are the result of the present calculation; squares represent experimental data from Ref. [3].

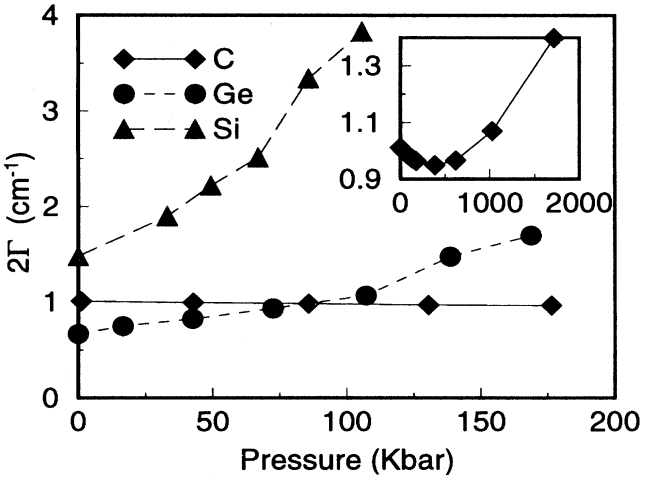

FIG. 3. Calculated pressure dependence of the Raman linewidths (2Γ) for C, Si, and Ge in the diamond structure. The inset shows results for C over a larger pressure range.

falling approximately midway between the BZ center and edge [this is where the LA phonon dispersions $\omega_{\mathrm{LA}}(\mathbf{q})$ reach the value $\omega_{\mathrm{LA}} = \omega_{\mathrm{LTO}}/2$]. The remaining contributions correspond to the LTO $\rightarrow$ LA + TA process, and come from wave vectors closer to the BZ edge, in all the directions from Γ to zone boundary except around the $\Gamma - L$ direction, where the frequency of the TA branch is so low that no matching LA frequency exists yielding $\omega_{\mathrm{TA}}(\mathbf{q}) + \omega_{\mathrm{LA}}(-\mathbf{q}) = \omega_{\mathrm{LTO}}$. A similar behavior is found also for Ge. The maps of Figs. 4(c) and 4(d) show that when the pressure increases new channels begin to contribute, namely, those related to wave vector regions around the K and L points. The analysis of the corresponding final state spectra indicates that these channels involve LO and TA modes as final states, which are now compatible with conservation laws owing to two combined pressure-induced effects: the increased LTO frequency and the decreased frequency of the TA branches. We conclude that the dependence of the phonon lifetime upon pressure (and likely upon other applied fields as well) is quasilinear as long as the overall kinematics does not change: When the applied field determines the opening of new decay channels otherwise closed, then a steep variation of the lifetime may occur.

Of course, the detailed numerical values of the phonon lifetime depend both on *kinematic* effects (i.e., on the existence of allowed decay channels) and on *dynamic* effects (i.e., on the magnitude of the matrix elements responsible for the instability of one-phonon states). The latter are given by the magnitude of the tensor of the third derivatives of the crystal energy with respect to atomic displacements. In order to assess the sensitivity of our results to an accurate evaluation of the latter, we have performed test calculations of the linewidths of Si and Ge by interchanging their third-order coupling coefficients

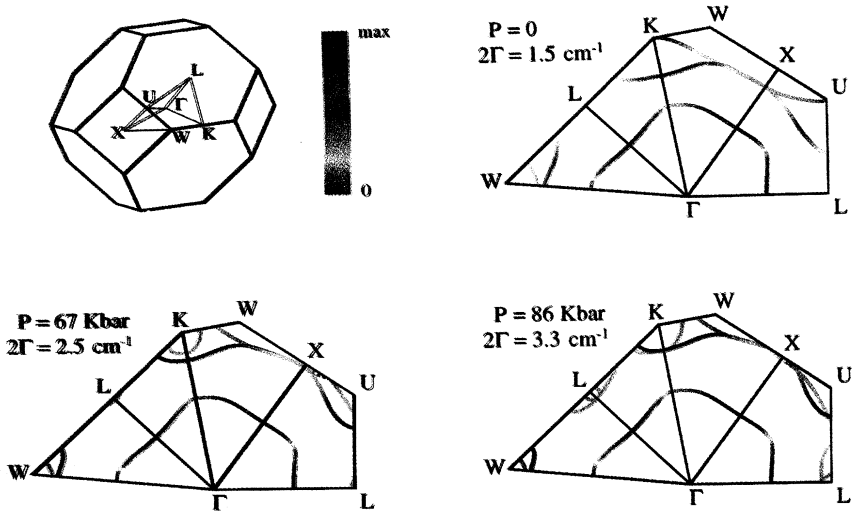

FIG. 4(color). Wave vector resolved final state spectra of Si (see text) at different pressures. (a) Sketch of the Brillouin zone; (b), (c), and (d) color maps at pressures $P = 0$, 67, and 86 kbar, respectively. The color scale goes from red to violet in order of increasing magnitude.

while leaving the kinematics (i.e., the phonon dispersions) unchanged. In spite of the similarities between the two materials, the results are affected by ~25%. We conclude that an accurate determination of the third-order anharmonic tensor is in general needed for a quantitative prediction of the lifetimes.

In summary, our results show that first-principles calculations of third-order interactions provide an accurate description of the anharmonic decay of phonons in semiconductors up to far above room temperature. Within density-functional perturbation theory, the required computational effort is comparable to that needed by standard lattice-dynamical calculations in the harmonic approximation. This opens the way to the prediction of anharmonic lifetimes in systems—such as some bulk compound semiconductors (e.g., AlAs) or heterostructures—where they are not easily accessed by experiments, and to the study of modifications, which can be induced by varying different applied fields and/or the characteristics of the samples by materials engineering.

[1] For a review see J. A. Kash and J. C. Tsang, in *Light Scattering in Solids VI,* edited by M. Cardona and G. Güntherodt (Springer, Berlin, 1991), p. 423.
[2] See, e.g., P. Lugli *et al.,* Phys. Rev. B **39**, 7852 (1989).
[3] J. Menéndez and M. Cardona, Phys. Rev. B **29**, 2051 (1984).
[4] For a review see M. Cardona *et al.,* J. Phys. Condens. Matter **5**, A61 (1993).
[5] P. G. Klemens, Phys. Rev. **148**, 845 (1966).
[6] R. A. Cowley, J. Phys. (Paris) **26**, 659 (1965).
[7] S. Narasimhan and D. Vanderbilt, Phys. Rev. B **43**, 4541 (1991).
[8] S. Baroni, P. Giannozzi, and A. Testa, Phys. Rev. Lett. **58**, 1861 (1987).
[9] P. Giannozzi *et al.,* Phys. Rev. B **43**, 7231 (1991).
[10] X. Gonze and J.-P. Vigneron, Phys. Rev. B **39**, 13 120 (1989).
[11] A. Dal Corso *et al.,* Phys. Rev. B **47**, 3588 (1993).
[12] P. Pavone *et al.,* Phys. Rev. B **48**, 3156 (1993).
[13] A. Debernardi and S. Baroni, Solid State Commun. **91**, 813 (1994).
[14] See, e.g., P. M. Morse and H. Feshbach, *Methods of Theoretical Physics* (McGraw-Hill, New York, 1953), Vol. II, p. 1120.
[15] Preliminary results were reported in A. Debernardi, S. Baroni, and E. Molinari, in *Proceedings of the 22nd International Conference on the Physics of Semiconductors,* edited by D. J. Lockwood (World Scientific, Singapore, 1994), p. 373. The present data are obtained with an improved convergence in the plane-wave expansion.
[16] R. S. Krishnan, Proc. Indian Acad. Sci. **24**, 45 (1946); S. A. Solin and A. K. Ramdas, Phys. Rev. B **1**, 1687 (1970); E. Anastassakis, H. C. Hwang, and C. H. Perry, Phys. Rev. B **4**, 2493 (1971); W. J. Borer, S. S. Mitra, and K. W. Namjoshi, Solid State Commun. **9**, 1377 (1971); R. M. Chrenko, J. Appl. Phys. **63**, 5873 (1988); M. A. Washington and H. Z. Cummins, Phys. Rev. B **15**, 5840 (1977); K. C. Hass *et al.,* Phys. Rev. B **44**, 12 046 (1991); J. Spitzer *et al.,* Solid State Commun. **88**, 509 (1993).
[17] (a) T. R. Hart, R. L. Aggarwal, and B. Lax, Phys. Rev. B **1**, 638 (1970); (b) R. Tubino, L. Piseri, and G. Zerbi, J. Chem. Phys. **56**, 1022 (1972); (c) P. A. Temple and C. E. Hathaway, Phys. Rev. B **7**, 3685 (1973); (d) M. Balkanski, R. F. Wallis, and E. Haro, Phys. Rev. B **28**, 1928 (1983); (e) Ref. [3].
[18] R. K. Ray, R. L. Aggarwal, and B. Lax, in *Light Scattering in Solids,* edited by M. Balkanski (Flammarion, Paris, 1971), p. 288; F. Cerdeira and M. Cardona, Phys. Rev. B **5**, 1440 (1972); Ref. [3]; H. D. Fuchs *et al.,* Phys. Rev. B **44**, 8633 (1991).

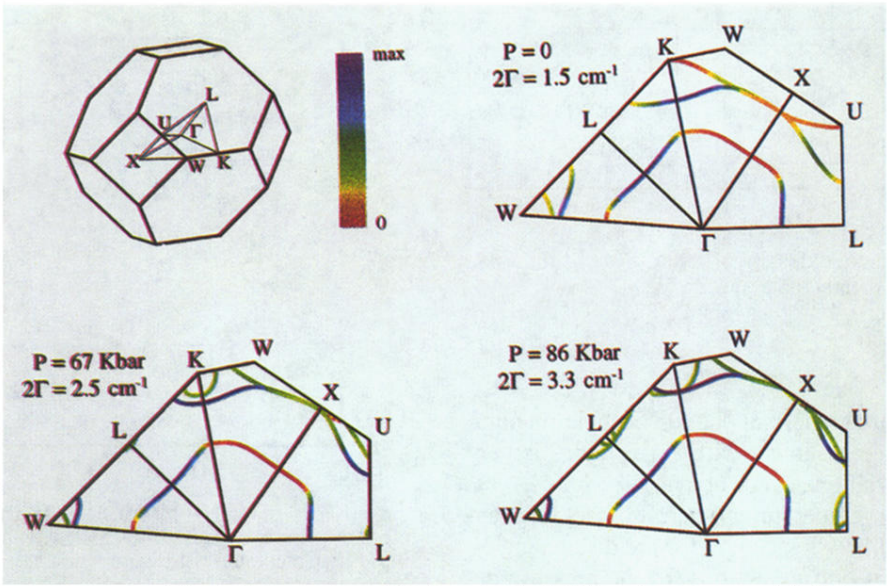

FIG. 4(color). Wave vector resolved final state spectra of Si (see text) at different pressures. (a) Sketch of the Brillouin zone; (b), (c), and (d) color maps at pressures $P = 0$, 67, and 86 kbar, respectively. The color scale goes from red to violet in order of increasing magnitude.